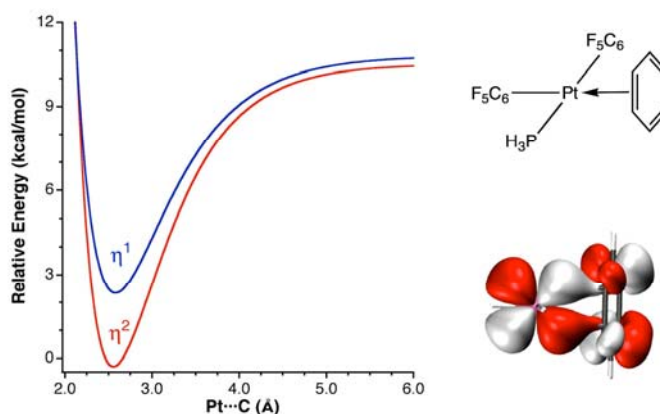


# Electronic and Structural Effects of Low Hapticity Coordination of Arene Rings to Transition Metals

Andrés Falceto,<sup>a</sup> Ernesto Carmona,<sup>b</sup> Santiago Alvarez<sup>a</sup>

<sup>a</sup>) Departament de Química Inorgànica and Institut de Química Teòrica i Computacional, Universitat de Barcelona, Martí i Franquès 1-11, 08028 Barcelona, Spain.

<sup>b</sup>) Instituto de Investigaciones Químicas and Departamento de Química Inorgánica, Universidad de Sevilla – Consejo Superior de Investigaciones Científicas, Av. Américo Vespucio 49, 41092 Sevilla, Spain.



## ABSTRACT

A DFT computational study and a structural analysis of the coordination of arenes to transition metals in low hapticity ( $\eta^1$  and  $\eta^2$ ) modes have been developed, including a pseudosymmetry analysis of the molecular orbitals and the introduction of a hapticity map that makes evident the different degrees of intermediate hapticities. Calculations on  $[\text{Pt}^{\text{II}}\text{L}_3(\text{C}_6\text{H}_6)]$  model complexes reveal a preference for the  $\eta^2$  mode, while the  $\eta^1$  coordination is found to be a low energy transition state for a haptotropic shift. The attachment of the arene to a side group that is coordinated to the metal introduces geometrical constraints which result in hapticities intermediate between one and two. Comparison of the  $\eta^1$  arene complexes with benzenium cations shows that in the former case the bonding to the metal involves essentially the  $\pi$  system of the arene, affecting only slightly the delocalized nature of the carbon-carbon bonds. This behavior is in sharp contrast with the frequently found  $\eta^1$  coordination of Cp that involves  $\sigma$  bonding and full dearomatization of the ring.

## Introduction

In recent years, a wide variety of compounds have been characterized in which one or two carbon atoms of an arene ring are in close contact with a transition metal, far from the  $\eta^6$  coordination that is found in the well-known sandwich and piano stool complexes. In spite of the wealth of structural data accumulated, there is no systematic study on the structural and electronic trends common to those low hapticity compounds. Many such complexes, for instance, appear in the literature and in the CSD (Cambridge Structural Database)<sup>1</sup> as forming a  $\sigma$  bond between the arene and the transition metal, others appear as non bonded, and only a fraction of them are represented as  $\pi$ -bonded arene complexes. An additional problem resides in the attribution of a hapticity number, since in many instances the differences in M-C distances do not allow one to decide which carbon atoms are truly bonded and which ones are not, hence situations intermediate between  $\eta^1$  and  $\eta^2$  or between  $\eta^1$  and  $\eta^3$  are quite common. Finally, there is a large number of complexes in which a pendant phenyl ring of a coordinated group (e.g., alkyl, aryl, phosphine or amine) may be close to the metal atom, thus raising doubts as to whether it is bonded or just sitting there.

Although we do not pretend to be comprehensive, we wish to provide a number of representative examples of cases in which a low hapticity coordination of an arene appears, starting by the independent rings, and looking afterwards at the anchored arene rings. Among the numerous examples of arene coordination to  $\text{Ag}^{\text{I}}$ , for instance, no clear preference is found for one or another hapticity.<sup>2</sup> Two nice examples of low hapticity coordination of independent benzene rings to a transition metal correspond to salts of the homoleptic cationic complex  $[\text{Ag}(\text{C}_6\text{H}_6)_3]^+$ . In one of them<sup>3</sup> the three benzene rings present an  $\eta^1$  coordination mode, in a second salt<sup>4</sup> one finds two  $\eta^1$ - and one  $\eta^2$ -coordinated rings, and in a third case<sup>5</sup> the three rings present an  $\eta^2$  mode. In a series of polyoxometalate-based coordination polymers, silver cations are coordinated by arene rings in  $\eta^1$ ,  $\eta^2$  and  $\eta^3$  coordination modes.<sup>6</sup> Independent arenes are also found coordinated to  $\text{Au}^{\text{I}}$ ,<sup>7</sup>  $\text{Zn}^{\text{II}}$ ,<sup>8</sup> and even to silylium cations.<sup>9</sup> In some instances an aryl group of a weakly coordinating  $\text{BAr}_4^-$  counterion can also be found coordinated with a low hapticity to  $\text{Sc}^{\text{III}}$ ,  $\text{Zr}^{\text{IV}}$  or  $\text{Cu}^{\text{I}}$ .<sup>10-12</sup>

Buchwald and coworkers have observed that the distal arene ring of coordinated biaryl phosphines often acts as an additional donor to palladium centers in an  $\eta^1$  or  $\eta^2$  mode, sometimes accompanied by dearomatization of that ring.<sup>13</sup> Similar  $\eta^1$  interactions have been found with  $\text{Au}^{\text{I}}$ ,<sup>14</sup>  $\text{Rh}^{\text{I}}$ ,<sup>15</sup>  $\text{V}^{\text{V}}$ ,<sup>16</sup> and  $\text{Pd}^0$  centers.<sup>17</sup> Anchored arenes coordinated in an  $\eta^2$  mode to  $\text{Rh}^{\text{I}}$ ,<sup>18</sup>  $\text{Ir}^{\text{I}}$ ,<sup>19</sup> and  $\text{Ru}^{\text{II}}$ <sup>20</sup> have also been described. Finally, low hapticity coordination

of biaryl groups is also common in the quintuply bonded  $\text{Ar}'\text{CrCrAr}'$  complexes reported by Power and co-workers ( $\text{Ar}' = \text{terphenyl ligand}$ ).<sup>21</sup> In related quadruply bonded molybdenum compounds obtained by the group of Carmona, one of the Mo atoms features a  $\text{Mo}\cdots\text{C}_{\text{arene}}$  interaction at a distance just slightly longer than the typical bond lengths in  $\pi$ -coordinated arene complexes.<sup>22</sup> Analogous  $\eta^1$  coordination from triaryl amido ligands have been reported in low coordinate  $\text{Co}^{\text{II}}$  and  $\text{Ni}^{\text{II}}$  complexes,<sup>23</sup> and the aryl ring of the neophyl group can also be found  $\eta^1$  coordinated to  $\text{Pd}^{\text{II}}$ .<sup>24</sup> Even if the coordinative bonding of those aryl rings could be questioned because they are held in close proximity to the metal center by the coordinated P, N or C atom, independent arene rings are indeed  $\eta^1$  coordinated in several cases described above.

We present in this work a combined computational and structural analysis of the  $\pi$ -coordination of arene rings to transition metals through only one or two carbon atoms, i.e., with  $\eta^1$  or  $\eta^2$  coordination modes. We show first how a phenyl ring can act as a  $\pi:\eta^1$ -bonded ligand by looking at its interaction with the simplest Lewis acid, the proton. We then present a hapticity map that allows for some degree of discrimination of the low hapticities ( $\eta^1$ ,  $\eta^2$  and  $\eta^3$ ) that will be useful for the subsequent discussion, and then present our computational results on the low hapticity coordination of a benzene ring to a  $\text{d}^8\text{-PtL}_3$  fragment, and compare them with the so called secondary coordination of flanking phenyl rings in  $\sigma$ -bonded bi- and ter-phenyl groups.

### **A simple model for mono-hapto coordination of phenyl rings**

The  $\pi$  coordination of an arene ring to a metal through a single carbon atom can be represented as a Lewis acid-base interaction (**1**). Its simplest expression consists in the protonation of a benzene ring to yield a benzenonium cation  $\text{C}_6\text{R}_6\text{H}^+$  (**2**), also called a Wheland intermediate. That interaction is made more efficient by localizing at the interacting carbon atom two of the six  $\pi$  electrons of benzene, forming a lone pair that can account for bonding with the proton. To that end, a reorganization of the  $\pi$  orbitals of the type shown in Figure 1 might be expected, resulting in an MO localized mostly at the interacting carbon. Such a localization is possible thanks to symmetry lowering from  $\text{D}_{6\text{h}}$  to  $\text{C}_s$ , whereupon the  $\text{a}_{2\text{u}}$  and one of the  $\text{e}_{1\text{g}}$  MOs become of the same symmetry ( $\text{A}'$ ). The overlap between the lone pair orbital and the Lewis acid can be further enhanced by an  $\text{sp}^3$  hybridization, which may result also in an out of plane shift of the R group, gauged by the angle  $\gamma$  defined in **2**. The angle formed by the incoming Lewis acid ( $\varphi$  in **2**) will allow us to calibrate the  $\pi$  ( $\varphi \approx 90^\circ$ ) or  $\sigma$  ( $\varphi \approx 55^\circ$ ) coordination in the  $\eta^1$  mode. The orbital localization is nicely illustrated by looking at

the gradual changes of the 1a' MO of benzene as the proton approaches an arene carbon atom (Figure 2).

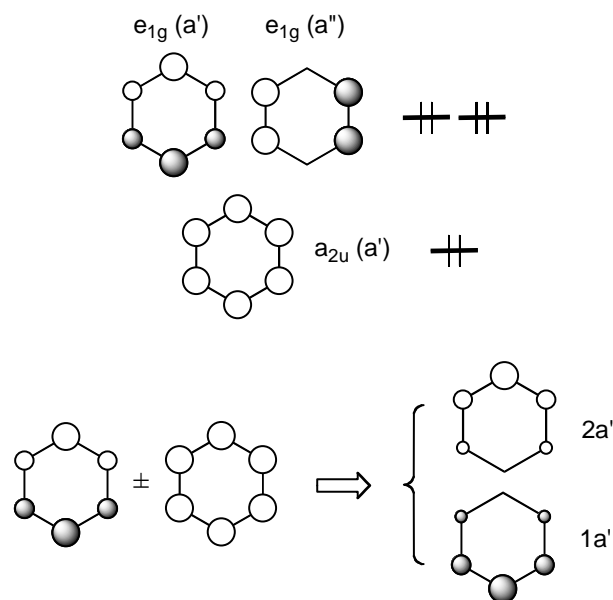


**Figure 1.** Occupied  $\pi$  molecular orbitals of benzene (above) and mixing upon symmetry descent (below) that localizes one of them at the carbon atom that interacts with a Lewis acid in an  $\eta^1$  mode.

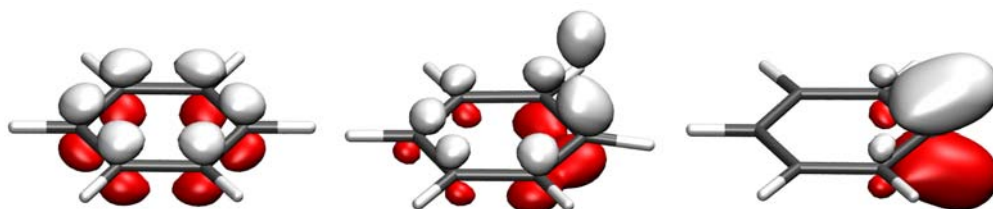
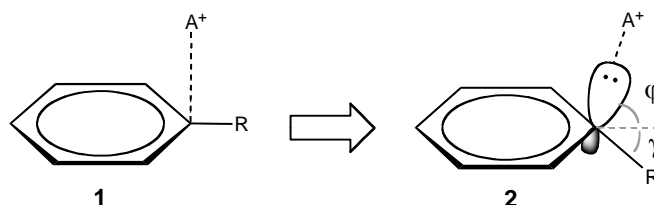
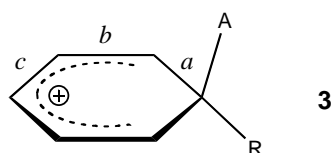


**Figure 2.** The  $\pi$ -type  $a_{2u}$  MO of benzene (left) and its progressive localization upon approaching a proton at 2.09 Å and  $\phi = 90^\circ$  (center), finally reaching the optimized structure of the  $C_6H_7^+$  benzenium cation (right).



The localization of the  $\pi$  orbitals can be described in terms of a Lewis structure of type 3, in which two of the  $\pi$  electrons become involved in the Ph-A bond while the remaining four

$\pi$  electrons and the positive charge are delocalized throughout the rest of the ring. Such dearomatized ring presents a characteristic distribution of C-C bond distances,  $a > c > b$ . The structural data for benzenium cations available from the CSD (R = H, Me; A = H, Me, Ph, CH<sub>2</sub>Cl; 19 structural data sets from 17 structures with acyclic C-R bonds) avail this description, with average ring distances of 1.46(3), 1.38(5) and 1.40(2) Å for  $a$ ,  $b$  and  $c$ , respectively. DFT calculations on the C<sub>6</sub>H<sub>7</sub><sup>+</sup> cation yield a similar bond distance distribution (1.469, 1.369 and 1.410 Å for  $a$ ,  $b$  and  $c$ , respectively). Moreover, a population analysis discloses a negative charge at C<sub>ipso</sub> of -0.20 when a proton is approached at 2.09 Å, to be compared with -0.02 at the *para* carbon atom and with -0.10 in neutral benzene. Although in the C<sub>6</sub>H<sub>7</sub><sup>+</sup> benzenium cation, in which groups A and R are equivalent, one expects a full sp<sup>3</sup> hybridization, with identical angles  $\varphi$  and  $\gamma$  (**2**) when A and R have different electronic characteristics, situations closer to a perpendicular bonding of the incoming Lewis acid may occur. In fact, the structurally characterized benzenium cations with different combinations of A and R substituents present an average asymmetry in the two angles  $\varphi$  and  $\gamma$  of 15°.



### Low Hapticities in Transition Metal Complexes

In the compounds of interest to this work the coordination of an aryl group to a metal is not always easy to classify as  $\eta^1$ ,  $\eta^2$  or  $\eta^3$ , and it is therefore convenient to try and find a way to roughly distinguish those low hapticities from each other. We therefore propose to calibrate the hapticity by comparing the three shortest M-C distances,  $d_1 < d_2 < d_3$  (Figure 3a) via the distance ratios  $\rho_1$  and  $\rho_2$  (equations 1 and 2) to put complexes with metal atoms of different size on the same scale.

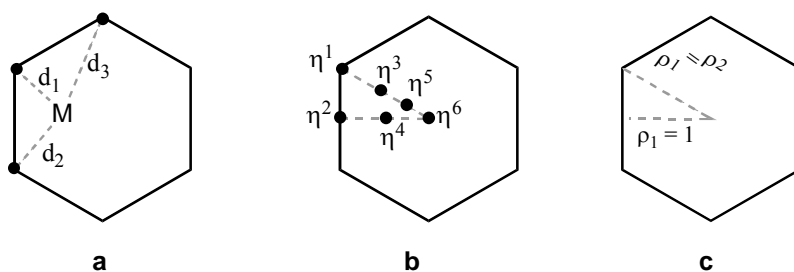


**Figure 3.** (a) Projection on the arene ring of the three shortest M-C distances in a low hapticity metal-arene coordination. (b) Projection of the positions of the metal atom corresponding to ideal hapticities. (c) Reference lines for hapticity maps.

$$\rho_1 = d_2/d_1 \quad [1]$$

$$\rho_2 = d_3/d_1 \quad [2]$$

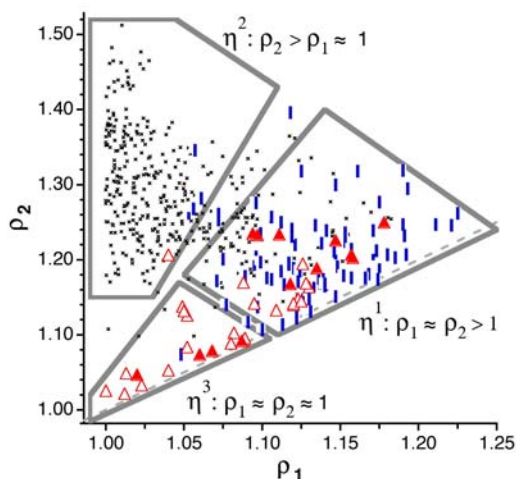


**Figure 4.** Hapticity map that represents the ratios of the three shortest M-C distances defined in equations 1-2 for arene complexes classified in the CSD as  $\eta^1$ - (bars),  $\eta^2$ - (small crosses) and  $\eta^3$ -coordinated (triangles; filled triangles for group 10 metal complexes). The limits of the regions ascribed to each hapticity are arbitrarily set. For data and references see Supporting Information (Tables S1-S3).

A projection of the ideal position of the metal atom on the arene ring for the different hapticities is shown in Figure 3b, and some special values of  $\rho_1$  and  $\rho_2$  are sketched in Figure 3c. Thus, for an  $\eta^3$  coordination, we expect the three M-C bond distances to be approximately equivalent and therefore  $\rho_1 \approx \rho_2 \approx 1$ . For an  $\eta^2$  coordination, for which  $d_1 \approx d_2 < d_3$ , we expect  $\rho_2 > \rho_1 \approx 1$ . Finally, for an  $\eta^1$  coordination the following relationship holds:  $\rho_1 \approx \rho_2 \gg 1$ . A scatterplot of the two ratios should therefore present distinct regions for the three hapticities, delimited by the polygons shown in Figure 4, whose boundaries have been arbitrarily established. We also show there the ratios for the experimental structures classified in the CSD as mono-, di- or tri-hapto (Tables S1-S3). It is seen that the classification criterion proposed works reasonably well for a large number of structures, even if there are no clear-cut borders. The dispersion of the points with the same hapticity along the diagonal is found to be correlated with the angle  $\varphi$  (2). This plot suggests that the hapticity proposed in some cases is inconsistent with the geometrical parameters. In particular, since the subsequent discussion will be focused mostly on group 10 complexes, we single out in Figure 4 the purported  $\eta^3$  compounds of those metals, and observe that those that fall on the  $\eta^1$  region of the hapticity map<sup>25,26</sup> obey the sixteen electron rule if they are considered as two-electron donors, whereas

those that appear in the  $\eta^3$  region<sup>27</sup> should be considered as allylic four-electron donors according to the electron counting rule. This example shows the hapticity parameters are in good agreement with bonding considerations.

It must be noted that a hapticity index proposed by Kochi,<sup>3,28</sup> defined assuming that the metal atom sits directly atop a C-C bond, allows one to discriminate  $\eta^1$  from  $\eta^2$  coordination, giving in all those cases values comprised between 1.0 and 2.0. However, that hapticity index is not applicable for higher hapticities. For instance, the  $\eta^3$ ,  $\eta^4$  and  $\eta^6$  coordination modes yield a Kochi hapticity index of 2. Similarly, the hapticity map used here is intended to discriminate the low hapticities ( $\eta^1 - \eta^3$ ), but is not applicable to higher hapticities, since the ratios for  $\eta^3$ ,  $\eta^5$  and  $\eta^6$  coordinations all fall along the  $\rho_1 = \rho_2$  line, with  $\rho_1 = \rho_2 = 1$  for the ideal  $\eta^6$  mode (Figure 3).

### Computational Study of $\eta^1$ Coordination of Benzene to a $d^8$ -PtL<sub>3</sub> Fragment

In the experimental structures of the compounds considered here the metal-carbon distances of the  $\eta^1$ -interacting phenyl groups are usually within the range found for  $\pi$ -bonded metal-olefin complexes. In addition, in some cases deviations of bond angles within the ligand from typical values can be interpreted as due to the tendency of the phenyl ring to bond to the metal, as discussed by Carmona et al.<sup>24</sup> for two palladium complexes described by them as  $\pi$ - $\eta^1$ -coordinated. In those compounds the phenyl ring bonds to a  $d^8$ -ML<sub>3</sub> fragment, thus completing a square planar coordination sphere, with M-C distances of 2.29 – 2.44 Å,<sup>24,29,30</sup> slightly longer than the sum of covalent radii (2.09 Å)<sup>31</sup> and significantly shorter than the sum of the van der Waals radii (3.06 Å).<sup>32</sup>

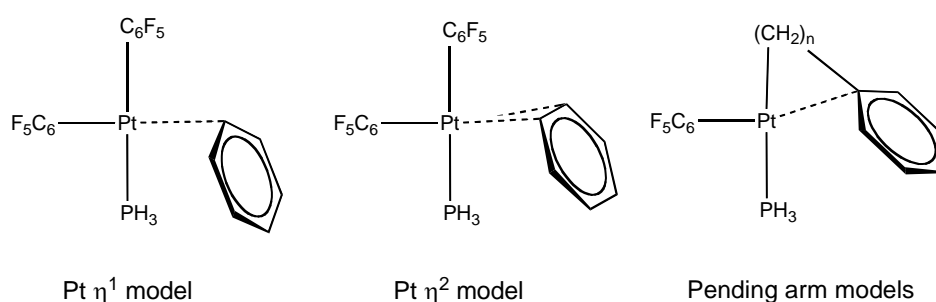


**Figure 5.** Computational models used to probe the  $\eta^1$  and  $\eta^2$  coordinations of a phenyl ring to a single metal atom center ( $n = 1 - 3$ ).

To probe the bonding nature of the  $\eta^1$  and  $\eta^2$  interactions of benzene towards mononuclear metal centers, we have performed DFT calculations on model platinum

complexes with independent and anchored phenyl rings, built up as simplified versions of well characterized Pd<sup>24</sup> and Pt<sup>30</sup> compounds (Figure 5). The first two models will allow us to explore the preferences of Pt for the  $\eta^1$  or  $\eta^2$  interaction with an independent benzene molecule, which may act in both cases as a two-electron donor to fulfill the 16-electron count required for a square planar platinum(II) ion. In a second set of models, the phenyl ring is brought to close proximity of the Pt atom by coordination of an alkyl arm of varying length. Those models might allow us to analyze the relationship of the span between the  $\sigma$ -coordinated carbon atom and the phenyl ring with the coordinating ability of the latter.

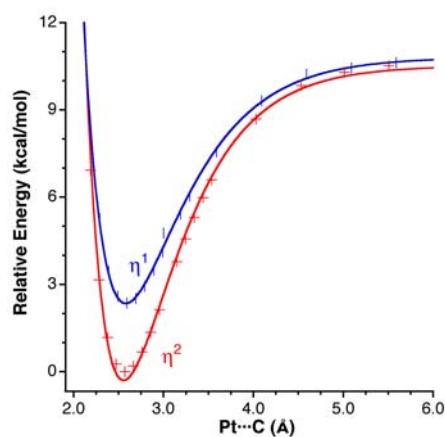


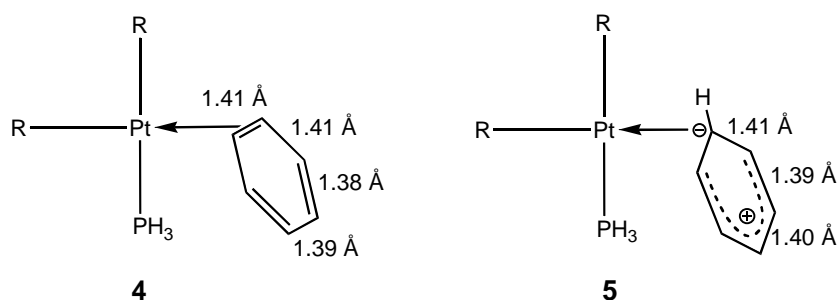
**Figure 6.** Energy of *cis*-[(F<sub>5</sub>C<sub>6</sub>)<sub>2</sub>(PH<sub>3</sub>)Pt(C<sub>6</sub>H<sub>6</sub>)] as a function of the shortest Pt-C(benzene) distance for the  $\eta^1$  and  $\eta^2$  coordination modes of benzene, relative to the optimized  $\eta^2$  geometry, with the orientation of the benzene molecule relative to the (C<sub>6</sub>F<sub>5</sub>)<sub>2</sub>(PH<sub>3</sub>)Pt fragment frozen as in the energy minimum.

Potential energy curves (see Computational Details) for the coordination of benzene to the model Pt fragment in both  $\eta^1$  and  $\eta^2$  modes, generated by single point calculations at fixed Pt-C distances with the rest of the geometry optimized, are shown in Figure 6. A fitting of the calculated energies to a Morse potential yields energy minima at Pt-C distances of 2.580 ( $\eta^1$ ) and 2.556 Å ( $\eta^2$ ). Upon full geometry optimization and vibrational analysis, we find the  $\eta^2$ -coordinated form to be an energy minimum at Pt-C = 2.568 Å and the  $\eta^1$ -one to be a transition state in-between two dihapto forms, setting a very small barrier for a fluxional haptotropic shift. The calculated dissociation energy of benzene from [Pt(C<sub>6</sub>F<sub>5</sub>)<sub>2</sub>(PH<sub>3</sub>)( $\eta^2$ -C<sub>6</sub>H<sub>6</sub>)] (see Computational Details) is 9.5 kcal/mol, significantly smaller than, but comparable to, the dissociation energy of ethylene from the analogous complex [Pt(C<sub>6</sub>F<sub>5</sub>)<sub>2</sub>(PH<sub>3</sub>)( $\eta^2$ -C<sub>2</sub>H<sub>4</sub>)] at the same computational level (14.6 kcal/mol). From these results we can conclude that the benzene molecule is effectively bonded to the metal atom, i.e., it acts as a two-electron donor



toward a metal fragment via an  $\eta^2$  coordination mode. When free from other constraints, this coordination mode is slightly favored, but one can expect that steric or geometrical constraints which prevent such a coordination mode could induce the alternative  $\eta^1$  coordination with only a small loss of bonding energy. The calculated dissociation energy of benzene from  $[\text{Pt}(\text{C}_6\text{F}_5)_2(\text{PH}_3)(\eta^1\text{-C}_6\text{H}_6)]$  is 8.5 kcal/mol, only 1.0 kcal/mol lower than that of the  $\eta^2$ -coordinated form. Note that the situation is reversed for the benzenium cation  $\text{C}_6\text{H}_7^+$ , for which the  $\eta^1$  structure is a global energy minimum and the  $\eta^2$  one is a transition state.<sup>33</sup>

The C-C bond distance distributions in the  $\eta^2$  energy minimum and the  $\eta^1$  transition state follow the trends expected for Lewis structures **4** and **5**, respectively, although the bond localization within the benzene ring is less pronounced than in the benzenium cation. Other geometrical parameters that witness the lesser perturbation of the arene ring by coordination to Pt, as compared to bonding to a proton, are the angles  $\varphi$  and  $\gamma$ . The shift from the ring plane of the hydrogen at the coordinated carbon atom is rather small in both hapticities ( $\gamma \approx 6 - 8^\circ$ ), and the ring is coordinated in a nearly perpendicular orientation, although with a significant difference between the  $\eta^1$  and  $\eta^2$  forms ( $\varphi = 77$  and  $97^\circ$ , respectively).



Next we introduce the model complexes  $[(\text{F}_5\text{C}_6)_2(\text{PH}_3)\text{Pt}(\{\text{CH}_2\}_n\text{Ph})]$ , in which a phenyl ring is attached to a coordinated Pt-( $\text{CH}_2$ )<sub>n</sub>-alkyl chain, with  $n = 1, 2$  or  $3$  (Figure 5, right). Their optimized geometries all have short Pt-C<sub>aryl</sub> distances (2.31, 2.49 and 2.55 Å for  $n = 1, 2$  and  $3$ , respectively). It is interesting to note that the shorter distances coexist with smaller  $\varphi$  angles (**2**), indicating the different affinity of the *ipso* carbon atom and the rest of the ring towards the metal atom. In the case of a  $\text{CH}_2\text{-CH}_2$  arm, that angle is practically identical to the one found for our model with an independent benzene molecule, yet the Pt-C distance is somewhat shorter for the anchored phenyl group.

If we compare now our computational models with related experimental structures regarding their position in a hapticity map, we find that the optimized benzene adducts of type **4** appear at the leftmost part of the  $\eta^2$  zone (Figure 7:  $\rho_1 = 1.00$ ,  $\rho_2 \approx 1.32$ ), in the same zone

occupied by a number of experimental structures, some of them very close to the calculated molecules.<sup>34</sup> The transition states (TS), on the other hand, appear clearly within the  $\eta^1$  region (Figure 7), close to several experimental structures of both independent and anchored group 10 metal complexes.<sup>26,35</sup> Finally, the model complexes in which a phenyl group is attached to  $\sigma$ -bonded  $(\text{CH}_2)_n$  groups appear at different positions depending on the length of the bridging alkyl group, but all within the  $\eta^2$  region, surrounded by many experimental structures of anchored aryl groups, some of them very close to our calculated structures, either in mononuclear,<sup>24,36,37</sup> or as bridging groups in metal-metal bonded complexes.<sup>37,38</sup> It is to be noted that two conformations of minimum energy have been found for  $[(\text{F}_5\text{C}_6)_2(\text{PH}_3)\text{Pt}(\text{CH}_2\text{Ph})]$ , which correspond to two alternative  $\eta^2$  coordinations of the arene ring.

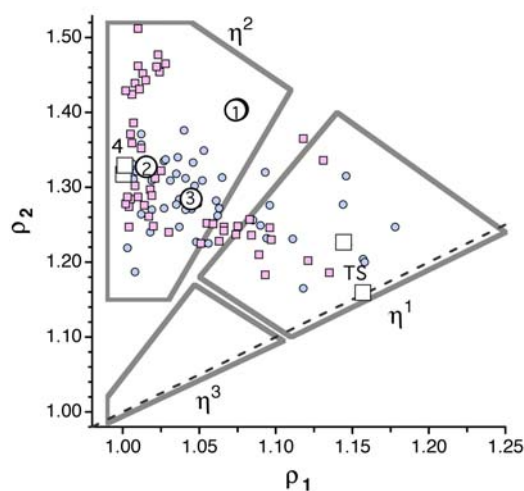


**Figure 7.** Hapticity map for the low hapticity phenyl rings in calculated Pt and experimental Ni, Pd, and Pt structures (see Figure 2 and equations 1-2 for definitions). Calculated structures for  $[(\text{F}_5\text{C}_6)_2(\text{PH}_3)\text{Pt}(\text{C}_6\text{H}_6)]$  and  $[(\text{H})_3\text{Pt}(\text{C}_6\text{H}_6)]^-$  are represented by empty squares, those of  $[(\text{F}_5\text{C}_6)_2(\text{PH}_3)\text{Pt}(\{\text{CH}_2\}_n\text{Ph})]$  by empty circles, with the value of  $n$  indicated inside the circle. The corresponding experimental structures of Ni, Pd and Pt complexes are represented by small filled squares (independent arenes) and circles (anchored arenes). For data and references see Supporting Information (Tables S4 and S5).

## Molecular Orbital Localization in $\eta^1$ - and $\eta^2$ -Platinum(II) Complexes.

As shown above for the simplest Lewis acid, the proton (Figures 1 and 2), coordination of benzene in a low hapticity mode to a transition metal may bring about significant localization of its  $\pi$  orbitals. Such a localization is the result of mixing of the  $a_{2u}$  and one of the degenerate  $e_{1g}$  benzene MOs, whereby the former achieves a significant degree of localization at one ( $\eta^1$ ) or two neighboring ( $\eta^2$ ) carbon atoms, as seen in Figure 8. It must be noted that, at difference with the proton, the transition metals have occupied d orbitals that may also interact with the benzene  $\pi$  system, thus disfavoring a degree of lone pair localization as extensive as found in the benzenium cation.

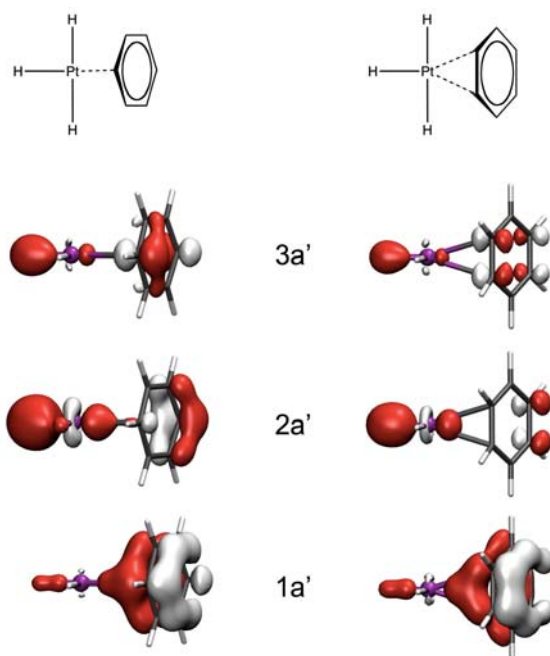


**Figure 8.** Localization of the occupied MOs of  $A'$  symmetry of  $[(H)_3Pt(C_6H_6)]^-$  built up from the benzene  $a_{2u}$  and  $e_{1g}$   $\pi$ -orbitals (Figure 1) and a metal  $pd$  hybrid in the  $\eta^1$  (left) and  $\eta^2$  (right) coordination modes.

The orbital localization upon symmetry descent from  $D_{6h}$  to  $C_s$  in  $[(H)_3Pt(C_6H_6)]^-$  can be traced back to contributions of the MO's of the free benzene molecule by means of a pseudosymmetry analysis.<sup>39</sup> Through such an analysis we can decompose each MO as a sum of contributions from functions belonging to the irreducible representations of the pseudosymmetry  $D_{6h}$  group, which is a local symmetry group for the benzene ring. The results (Table 1) tell us that the lowest  $1a'$  MO in both coordination modes is mostly the  $a_{2u}$

orbital of benzene, while the 2a' and 3a' occupied orbitals are mostly mixtures of a benzene  $e_{1g}$  orbital and the metal pd hybrid, as can be seen in Figure 8. We wish to stress how a small degree of mixing of  $a_{2u}$  and  $e_{1g}$  orbitals induce a significant degree of localization. It is also noteworthy that the metal atom strongly polarizes the lowest 1a' MO, although the resulting geometric effect on the benzene ring is small. A qualitatively similar picture results from a pseudosymmetry analysis of the more realistic model *cis*-[(F<sub>5</sub>C<sub>6</sub>)<sub>2</sub>(PH<sub>3</sub>)Pt(C<sub>6</sub>H<sub>6</sub>)], even if the quantitative description is now reversed (see Supporting Information, Table S6), with the metal (and C<sub>6</sub>F<sub>5</sub> ligands) participating mostly in the 1a' and 2a' MO,s and the 3a' orbital being composed to a greater proportion of the benzene  $e_{1g}$  orbital.

**Table 1.** Orbital contributions (in percentages) of the three occupied  $\pi$ -type MOs of benzene and the xz-type orbital in [H<sub>3</sub>Pt( $\eta^1$ -C<sub>6</sub>H<sub>6</sub>)]<sup>-</sup> and [H<sub>3</sub>Pt( $\eta^2$ -C<sub>6</sub>H<sub>6</sub>)]<sup>-</sup>, in terms of irreducible representations of the D<sub>6h</sub> pseudosymmetry group.

MO	D <sub>6h</sub> representation			
	E <sub>1g</sub>	A <sub>2u</sub>	E <sub>2u</sub>	Other
[H <sub>3</sub> Pt( $\eta^1$ -C <sub>6</sub> H <sub>6</sub> )] <sup>-</sup> 1a'	1	91	1	7
2a'	38	14	8	40
3a'	62	6	6	26
1a''	94	0		6
[H <sub>3</sub> Pt( $\eta^2$ -C <sub>6</sub> H <sub>6</sub> )] <sup>-</sup> 1a'	2	85	1	12
2a'	38	13	9	40
3a'	63	5	7	25
1a''	90	0	3	7
2a''	36	0	35	29

The higher stability of the  $\eta^2$  coordination mode in a Pt complex is explained by the presence of the symmetry-allowed back donation of the  $d_{xz}$  pair of electrons to one the  $e_{2u}$  antibonding  $\pi$  orbitals of benzene (Figure 9). In fact, the symmetry of the complex is so low that this MO (2a'') mixes three benzene  $\pi$  orbitals in a bonding combination that belongs to the A'' symmetry representation of the C<sub>s</sub> point group:  $b_{1g}$  (10%, included in the "Other" column of Table 1) and one orbital from each of the  $e_{2u}$  and  $e_{1g}$  sets.

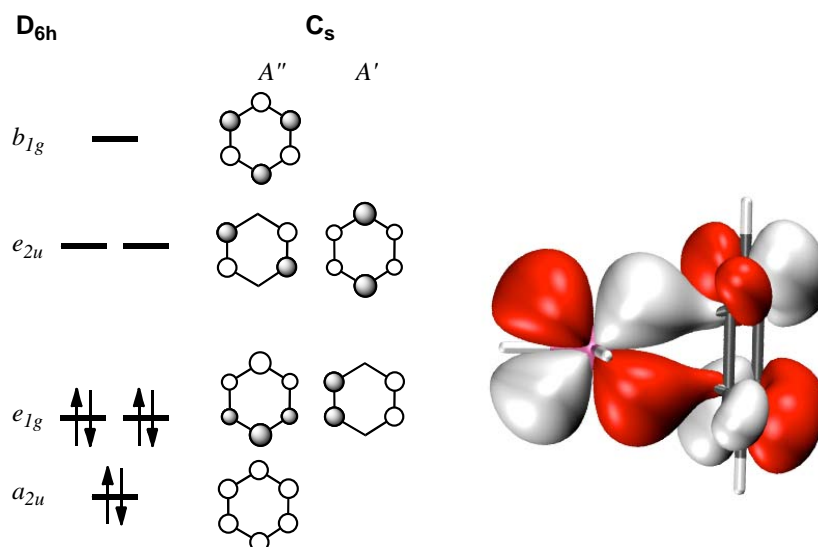


**Figure 9.** *Left:* Symmetry representations of the  $\pi$  orbitals of benzene upon symmetry descent to the  $C_s$  point group due to its  $\eta^2$  coordination to Pt. *Right:* Occupied  $2a''$  molecular orbital in  $[H_3Pt(\eta^2-C_6H_6)]^-$  showing the back-bonding interaction.

## Discussion

Unlike the benzenium cations, the calculated Pt complexes show a preference of the arene ring for an  $\eta^2$  coordination, while the  $\eta^1$  mode corresponds to a bonded transition state for a haptotropic shift between two neighboring C-C bonds. In both coordination modes there is a moderate bonding energy consistent with the existence of a coordinative bond between the arene and the metal.

A topological analysis of the electron density shows in most of our calculated complexes a bond critical point between the metal atom and the  $\eta^1$ -coordinated carbon atom of the phenyl ring, and two M-C bond critical points for the  $\eta^2$ -coordinated species. The exceptions are the complexes  $[(F_5C_6)_2(PH_3)Pt(\{CH_2\}_nPh)]$  with  $n = 1, 2$ , for which no Pt-C bond critical point has been found. The analogous compound with a larger spacer between the alkyl and phenyl groups ( $n = 3$ ), however, also presents a Pt-C bond critical point with the phenyl ring, even if the Pt-C distances are larger. The electron densities at the bond critical point present values within the range 0.03 – 0.05.

Calculated Wiberg bond indices of the order of 0.1 - 0.2 for the M-C contact in the  $\eta^1$ -coordinated species are consistent with the existence of bonding. Moreover, bond orders of around 0.05 - 0.10 with the two neighboring carbon atoms indicate that the electron pair

involved in the donation towards the metal atom is not fully localized and that electronically the coordination has a small  $\eta^3$ -character, in spite of the geometrical hapticity discussed above. For the  $\eta^2$ -bonded species the Wiberg bond indices also have similar values for the two M-C bonds (between 0.1 and 0.2), except for  $[(F_5C_6)_2(PH_3)Pt(CH_2Ph)]$  that presents two distinct bond indices of 0.20 and 0.13, consistent with its hapticity being intermediate between one and two or, equivalently, with two significantly different Pt-C bond distances.

The preference for the  $\eta^2$  coordination of an independent benzene molecule to a platinum(II) center is consistent with the experimental structural data. We carried out a structural database search for group 10 metal complexes  $\eta^2$ - or  $\eta^1$ -coordinated by independent or anchored arene rings. When the arene is in contact with a  $d^8$ - $ML_3$  fragment ( $M = Pd, Pt$ ), the M-C distance is within the ranges 2.22-2.45 and 2.11-2.52 Å for the  $\eta^1$  and  $\eta^2$  coordinated arenes, respectively, just slightly longer in average than the distances found in the related ethylene complexes (2.05-2.29 Å). In contrast, in some cases in which an anchored arene sits on top of an axial position of a  $d^8$ - $ML_4$  complex ( $M = Pd^{40}$  or  $Pt^{41}$ ), it appears to be weakly coordinated at M-C distances of 2.82 Å or longer.

Independent arenes coordinated in an  $\eta^1$  mode are also found for early transition metal ions, such as  $Sc^{III}$ ,<sup>10</sup>  $Ti^{IV}$ ,<sup>42</sup> or  $Zr^{IV}$ ,<sup>11</sup> all of them  $d^0$  ions that cannot back-bond to the arene, which we have seen that is the factor that favors  $\eta^2$  coordination. Finally, there are many examples of arene coordination to  $Ag^I$  and  $Cu^I$  cations, with either mono- or di-hapticity. It is likely that the core-like nature of the d electrons in the silver cation minimizes the back-bonding interaction that favors the  $\eta^2$  coordination. To check the coordinative preferences for an arene toward silver, we have optimized the structure of the  $[Ag(CNMe)_3(C_6H_6)]^+$  cation, and found a minimum for the  $\eta^1$  coordination. The  $\eta^2$  coordinated form was found to be a transition state between two equivalent  $\eta^1$  minima with a relative energy of 2.4 kcal/mol. Such a flat potential energy surface for the haptotropic shift is consistent with the existence of silver-arene adducts in both  $\eta^1$  and  $\eta^2$  coordination modes.

There are two relevant aspects of the  $\eta^1$  and  $\eta^2$  coordination of arenes to transition metals that deserve a more detailed discussion. One is the  $sp^3$  or p nature of the carbon orbital involved in the ring-metal interaction, the other the loss of the delocalized nature of the arene ring. We have seen that when we take a proton as a Lewis acid, bonding to an arene results in a  $\sigma$  C-H bond. Therefore, the carbon atom adopts an  $sp^3$  hybridization, resulting in angles  $\varphi$  and  $\gamma$  (**2**) of similar values. This result appears not only in our calculations, but also in the structures of benzenium cations, as seen in Figure 10. In contrast, the  $\eta^1$  arenes bond to transition metals in a direction practically perpendicular to the ring, with angles  $\varphi$  clustered

around 90°. At the same time, the substituent at the coordinated carbon atom deviates very little from the plane of the ring, with rather small angles  $\gamma$ . These data clearly indicate that the  $\eta^1$  coordination of arenes occurs through the  $\pi$  system, unlike the well known  $\eta^1$ -Cp complexes that form  $\sigma$  M-C bonds.

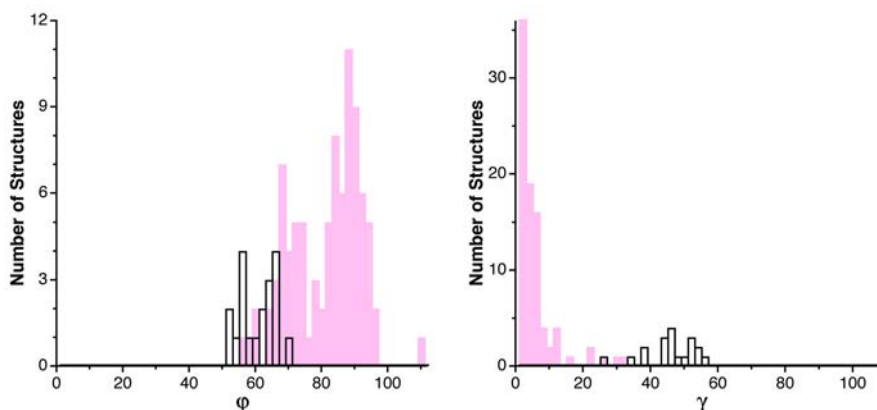


**Figure 10.** Distribution of angles  $\phi$  and  $\gamma$  in the experimental structures of benzonium cations<sup>43</sup> (white bins) and in the experimental structures of  $\eta^1$  arene complexes (shaded bins).

As for the loss of delocalization of the arene ring, the coordination to a transition metal has in general a much lesser effect than the formation of a benzonium cation, specially in the  $\eta^1$  coordination mode (Table 2). However, in specific cases small values of the angle  $\phi$  and C-C bond distance differences of the order of 0.04 Å seem to reveal a coordination intermediate between pure  $\sigma$  and pure  $\pi$ , as in some benzyl complexes,<sup>44</sup> that can be schematically represented by the Lewis structure **3**. The  $\eta^2$ -coordinated arenes show in general a clearer localization of their C-C bonds according to the Lewis structure **6**: the coordinated bond  $r$  is longer than expected for a double bond due to its coordination as rationalized by the Dewar-Chatt-Duncanson model, but the two other double bonds,  $t$ , are clearly shorter than the formal single bonds  $s$  and  $u$ .

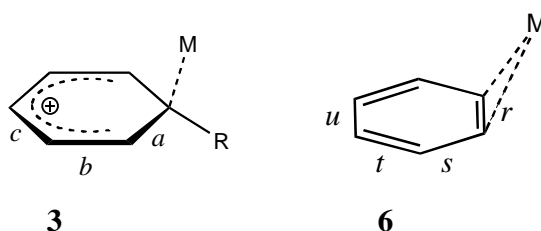


**Table 2.** Average of the experimental C-C distances (in Å) of arene rings in benzonium cations and in arenes  $\eta^1$  and  $\eta^2$ -coordinated to transition metals.

C-C dist.	Benzonium	$\eta^1$ arenes	$\eta^2$ arenes
<i>a</i>	1.46 (3)	1.39 (2)	
<i>b</i>	1.38 (5)	1.39 (1)	
<i>c</i>	1.40 (2)	1.38 (1)	
<i>r</i>			1.40 (3)
<i>s</i>			1.41 (3)
<i>t</i>			1.38 (2)
<i>u</i>			1.40 (4)

### Concluding Remarks

The interaction of an arene ring in an  $\eta^1$  mode to a Lewis acid results in an orbital localization of one  $\pi$  electron pair at the interacting carbon atom and alters the carbon-carbon bond delocalization. When the Lewis acid is a transition metal, the electron counting rules are consistent with two-electron donation from an  $\eta^1$  coordinated arene to  $d^8$ -ML<sub>3</sub> or  $d^6$ -ML<sub>5</sub> fragments. Although arenes act as two-electron donors in both  $\eta^1$  and  $\eta^2$  coordination modes, the latter is preferred in electron precise complexes, according to our calculations in a model Pt complex, because of the back bonding interaction of an occupied d orbital. The  $\eta^1$  coordination may appear in Rh, Ir, Ni, Pd and Pt complexes due to the geometrical constraints imposed by an anchored arene.

Low hapticity arene coordination to  $d^0$  metals devoid of back-bonding seems to favor  $\eta^1$  coordination. Also the  $d^{10}$  ions Ag<sup>I</sup> and Cu<sup>I</sup> seem to have no special preference between  $\eta^1$  and  $\eta^2$  coordination. The MO and structural analysis presented here allows us to conclude that the  $\eta^1$  coordination of arenes is truly a  $\pi$ -type coordination, at difference with the  $\sigma$ -type  $\eta^1$  coordination of Cp. The similar bonding patterns found for independent and anchored arenes point to true coordinative  $\eta^1$  or  $\eta^2$  bonding of flanking arenes in metal-metal multiply bonded complexes, in which these arene rings have been often said to present "secondary interactions" or to just provide steric protection.



## Computational Details

All the calculations have been obtained at the density functional theory (DFT) level using the B3LYP exchange-correlation functional with the help of the Gaussian 09 suite of programs.<sup>45</sup> Optimized molecular geometries have been obtained with the 6-311G(d,p) basis set for all atoms except for Pt for which relativistic Stuttgart/Dresden pseudopotentials and the SDD basis set was used. The analysis of the vibrational frequencies has been carried out within the harmonic approximation. The potential energy curves for the dissociation of the benzene ring and the metal fragment as well as the BSSE-corrected interaction energies were calculated performing single point calculations on the optimized geometries with the SARC-ZORA all-electron basis set for Pt.<sup>46</sup> Optimization of the lowest energy structure of  $[\text{Pt}(\text{C}_6\text{F}_5)_2(\text{PH}_3)(\eta^2\text{-C}_6\text{H}_6)]$  of Figure 6 with the SDD basis set led to a minimum with the benzene ring sitting on top of the  $\text{PH}_3$  ligand characterized by a vibrational analysis, whereas optimization of the  $\eta^1$  form led to a transition state characterized by one negative frequency. An alternative  $\eta^2$  geometry with the benzene ring facing one of the  $\text{C}_6\text{F}_5$  ligands was found to be also an energy minimum, barely 2.4 kcal/mol higher in energy than the other isomer. To calibrate the calculated interaction energies between the benzene molecule and the platinum fragments obtained with the SDD basis set, ZORA calculations were performed on both structures and BSSE-corrected dissociation energies of 8.5 and 9.5 kcal/mol were obtained for the  $\eta^1$  and  $\eta^2$  structures, respectively. Topological analyses of the electron density have been carried out with the AIMAll software.<sup>47</sup>

## Acknowledgments

Financial support from the Spanish Ministry of Science and Innovation (Projects CTQ2013–42501-P, CTQ2011–23862-C02-01 and Consolider-Ingenio 2010 CSD2007-00006), the Generalitat de Catalunya (Project 2009SGR-1459), and the Junta de Andalucía (Project P09-FQM-5117) is gratefully acknowledged.

## Supporting Information Available

Metal-arene distances and hapticity indices for transition metal complexes with arenes classified as  $\eta^1$ ,  $\eta^2$  or  $\eta^3$  in the CSD (data represented in Figures 4 and 7), pseudosymmetry analysis of some MOs for  $[(\text{F}_5\text{C}_6)_2(\text{PH}_3)\text{Pt}(\text{C}_6\text{H}_6)]$ , and atomic coordinates for optimized structures of the  $\text{C}_6\text{H}_7^+$  benzenonium cation,  $[\text{Pt}(\text{C}_6\text{F}_5)_2(\text{PH}_3)(\eta^2\text{-C}_6\text{H}_6)]$  (2 isomers),  $[\text{Pt}(\text{C}_6\text{F}_5)_2(\text{PH}_3)(\eta^1\text{-C}_6\text{H}_6)]$  (transition state),  $[(\text{F}_5\text{C}_6)_2(\text{PH}_3)\text{Pt}(\text{CH}_2\text{Ph})]$  (conformations A and B),  $[(\text{F}_5\text{C}_6)_2(\text{PH}_3)\text{Pt}(\{\text{CH}_2\}_2\text{Ph})]$ ,  $[(\text{F}_5\text{C}_6)_2(\text{PH}_3)\text{Pt}(\{\text{CH}_2\}_3\text{Ph})]$ ,  $[\text{Ag}(\text{CNMe})_3(\eta^1\text{-$

$C_6H_6]^+$ , and  $[Ag(CNMe)_3(\eta^2-C_6H_6)]^+$  (transition state). This material is available free of charge via the Internet at <http://pubs.acs.org>.

## References

- (1) Allen, F. H. *Acta Cryst.* **2002**, *B58*, 380.
- (2) Lindeman, S. V.; Rathore, R.; Kochi, J. K. *Inorg. Chem.* **2000**, *39*, 5707.
- (3) Ogawa, K.; Kitagawa, T.; Ishida, S.; Komatsu, K. *Organometallics* **2005**, *24*, 4842.
- (4) Batsanov, A. S.; Crabtree, S. P.; Howard, J. A. K.; Lehmann, C. W.; Kilner, M. J. *Organomet. Chem.* **1998**, *550*, 59.
- (5) Brasey, T.; Buryak, A.; Scopelliti, R.; Severin, K. *Eur. J. Inorg. Chem.* **2004**, 964.
- (6) Liang, M.-X.; Ruan, C.-Z.; Sun, D.; Kong, X.-J.; Ren, Y.-P.; Long, L.-S.; Huang, R.-B.; Zheng, L.-S. *Inorg. Chem.* **2014**, *53*, 897.
- (7) Weber, S. G.; Rominger, F.; Straub, B. F. *Eur. J. Inorg. Chem.* **2012**, 2863.
- (8) Guerrero, A.; Martin, E.; Hughes, D. L.; Kaltsoyannis, N.; Bochmann, M. *Organometallics* **2006**, *25*, 3311.
- (9) Wehmschulte, R. J.; Laali, K. K.; Borosky, G. L.; Powell, D. R. *Organometallics* **2014**, *33*, 2146.
- (10) Demir, S.; Lorenz, S. E.; Fang, M.; Furche, F.; Meyer, G.; Ziller, J. W.; Evans, W. J. *J. Am. Chem. Soc.* **2010**, *132*, 11151.
- (11) Cano, J.; Royo, P.; Jacobsen, H.; Blacque, O.; Berke, H.; Herdtweck, E. *Eur. J. Inorg. Chem.* **2003**, 2463.
- (12) Pasquali, M.; Floriani, C.; Gaetani-Manfredotti, A. *Inorg. Chem.* **1980**, *19*, 1191.
- (13) Milner, P. J.; Maimone, T. J.; Su, M.; Chen, J.; Müller, P.; Buchwald, S. L. *J. Am. Chem. Soc.* **1012**, *134*, 19922; Barder, T. E.; Buchwald, S. L. *J. Am. Chem. Soc.* **1007**, *129*, 12003.
- (14) Herrero-Gómez, E.; Nieto-Oberhuber, C.; López, S.; Benet-Buchholz, J.; Echavarren, A. M. *Angew. Chem. Int. Ed.* **2006**, *45*, 5455; Partyka, D. V.; Robilotto, T. J.; Zeller, M.; Hunter, A. D.; Gray, T. G. *Organometallics* **2008**, *27*, 28; Pérez-Galán, P.; Delpont, N.; Herrero-Gómez, E.; Maseras, F.; Echavarren, A. M. *Chem. Eur. J.* **2010**, *16*, 5324.
- (15) O'Connor, A. R.; Kaminsky, W.; Heinekey, D. M.; Goldberg, K. I. *Organometallics* **2011**, *30*, 2105.

- (16) Otten, E.; Batinas, A. A.; Meetsma, A.; Hessen, B. *J. Am. Chem. Soc.* **2009**, *131*, 5289.
- (17) Reid, S. M.; Boyle, R. C.; Mague, J. T.; Fink, M. J. *J. Am. Chem. Soc.* **2003**, *125*, 7816.
- (18) Liu, Z.; Yamamichi, H.; Madrahimov, S. T.; Hartwig, J. F. *J. Am. Chem. Soc.* **2011**, *133*, 2772.
- (19) O'Connor, A. R.; Kaminsky, W.; Chan, B. C.; Heinekey, D. M.; Goldberg, K. I. *Organometallics* **2013**, *32*, 4016.
- (20) Geldbach, T. J.; Pregosin, P. S. *Eur. J. Inorg. Chem.* **2002**, 1907.
- (21) Nguyen, T.; Sutton, A. D.; Brynda, M.; Fettinger, J. C.; Long, G. J.; Power, P. P. *Science* **2005**, *310*, 844; Wolf, R.; Ni, C.; Nguyen, T.; Brynda, M.; Long, G. J.; Sutton, A. D.; Fischer, R. C.; Fettinger, J. C.; Hellman, M.; Pu, L.; Power, P. P. *Inorg. Chem.* **2007**, *46*, 11277.
- (22) Carrasco, M.; Faust, M.; Peloso, R.; Rodríguez, A.; López-Serrano, J.; Alvarez, E.; Maya, C.; Power, P. P.; Carmona, E. *Chem. Commun.* **2012**, *48*, 3954; Carrasco, M.; Mendoza, I.; Álvarez, E.; Gurrane, A.; Maya, C.; Peloso, R.; Rodríguez, A.; Falceto, A.; Alvarez, S.; Carmona, E. *Chem. Eur. J.* **2014**, submitted; Carrasco, M.; Mendoza, I.; Faust, M.; López-Serrano, J.; Peloso, R.; Rodríguez, A.; Álvarez, E.; Maya, C.; Power, P. P.; Carmona, E. *J. Am. Chem. Soc.* **2014**, *136*, 9173.
- (23) Bryan, A. M.; Merrill, W. A.; Reiff, W. M.; Fettinger, J. C.; Power, P. P. *Inorg. Chem.* **2012**, *51*, 3366.
- (24) Cámpora, J.; López, J. A.; Palma, P.; Valerga, P.; Spillner, E.; Carmona, E. *Angew. Chem. Int. Ed.* **1999**, *38*, 147.
- (25) Gorlov, M.; Fischer, A.; Kloo, L. *J. Organomet. Chem.* **2004**, *689*, 489; Ito, M.; Matsumoto, T.; Tatsumi, K. *Inorg. Chem.* **2009**, *48*, 2215.
- (26) Christmann, U.; Vilar, R.; White, A. J. P.; Williams, D. J. *Chem. Commun.* **2004**, 1294; Gorlov, M.; Fischer, A.; Kloo, L. *Inorg. Chim. Acta* **2003**, *350*, 449; Christmann, U.; Pantazis, D. A.; Benet-Buchholz, J.; McGrady, J. E.; Maseras, F.; Vilar, R. *J. Am. Chem. Soc.* **2006**, *128*, 6376.
- (27) Thomas, J. C.; Peters, J. C. *J. Am. Chem. Soc.* **2003**, *125*, 8870; Jones, C.; Schulten, C.; Fohlmeister, L.; Stasch, A.; Murray, K. S.; Moubaraki, B.; Kohl, S.; Ertem, M. Z.; Gagliardi, L.; Cramer, C. J. *Chem. Eur. J.* **2011**, *17*, 1294; Dong, Q.; Zhao, Y.; Su, Y.; Su, J.-H.; Wu, B.; Yang, X.-J. *Inorg. Chem.* **2012**, *51*, 13162.

- (28) Vasilyev, A. V.; Lindeman, S. V.; Kochi, J. K. *Chem. Commun.* **2001**, 909.
- (29) Terheijden, J.; van Koten, G.; Vinke, I. C.; Spek, A. L. *J. Am. Chem. Soc.* **1985**, *107*, 2891; Cámpora, J.; Gutiérrez-Puebla, E.; López, J. A.; Monge, A.; Palma, P.; del Río, D.; Carmona, E. *Angew. Chem. Int. Ed.* **2001**, *40*, 3641.
- (30) Casas, J. M.; Forniés, J.; Martínez, F.; Rueda, A. J.; Tomás, M.; Welch, A. J. *Inorg. Chem.* **1999**, *38*, 1529.
- (31) Cordero, B.; Gómez, V.; Platero-Prats, A. E.; Revés, M.; Echeverría, J.; Cremades, E.; Barragán, F.; Alvarez, S. *Dalton Trans.* **2008**, 2832.
- (32) Alvarez, S. *Dalton Trans.* **2013**, *42*, 8617.
- (33) Solcà, N.; Dopfer, O. *Angew. Chem. Int. Ed.* **2002**, *41*, 3628.
- (34) Reinartz, S.; White, P. S.; Brookhart, M.; Templeton, J. L. *J. Am. Chem. Soc.* **2001**, *123*, 12724; Stromnova, T. A.; Dayneko, M. V.; Churakov, A. V.; Kuz'mina, L. G.; Cámpora, J.; Palma, P.; Carmona, E. *Inorg. Chim. Acta* **2006**, *359*, 1613; Norris, C. M.; Reinartz, S.; White, P. S.; Templeton, J. L. *Organometallics* **2002**, *21*, 5649; Stromnova, T. A.; Paschenko, D. V.; Boganova, L. I.; Daineko, M. V.; Katsner, S. B.; Churakov, A. V.; Kuz'mina, L. G.; Howard, J. A. K. *Inorg. Chim. Acta* **2003**, *350*, 283.
- (35) Catellani, M.; Mealli, C.; Motti, E.; Paoli, P.; Pérez-Carreño, E.; Pregosin, P. S. *J. Am. Chem. Soc.* **2002**, *124*, 4336.
- (36) Mikhel, I. S.; Ruegger, H.; Butti, P.; Camponovo, F.; Huber, D.; Mezzetti, A. *Organometallics* **2008**, *27*, 2937; Chai, D. I.; Thansandote, P.; Lautens, M. *Chem. Eur. J.* **2011**, *17*, 8175; Faller, J. W.; Sarantopoulos, N. *Organometallics* **2004**, *23*, 2008.
- (37) Zeng, B.-S.; Yu, X.; Siu, P. W.; Scheidt, K. A. *Chem. Sci.* **2014**, *5*, 2277.
- (38) Tatsumi, Y.; Naga, T.; Nakashima, H.; Murahashi, T.; Kurosawa, H. *Chem. Commun.* **2004**, 1430; Christmann, U.; Pantazis, D. A.; Benet-Buchholz, J.; McGrady, J. E.; Maseras, F.; Vilar, R. *Organometallics* **2006**, *25*, 5990; Ara, I.; Falvello, L. R.; Forniés, J.; Lalinde, E.; Martín, A.; Martínez, F.; Moreno, M. T. *Organometallics* **1997**, *16*, 5392; Omondi, B.; Shaw, M. L.; Holzapfel, C. W. *J. Organomet. Chem.* **2011**, *696*, 3091; Kannan, S.; James, A. J.; Sharp, P. R. *J. Am. Chem. Soc.* **1998**, *120*, 215; Barder, T. E. *J. Am. Chem. Soc.* **2006**, *128*, 898; Li, C.-S.; Cheng, C.-H.; Liao, F.-L.; Wang, S.-L. *Chem. Commun.* **1991**, 710.
- (39) Casanova, D.; Alemany, P.; Falceto, A.; Carreras, A.; Alvarez, S. *J. Comput. Chem.* **2013**, *34*, 1321; Falceto, A.; Casanova, D.; Alemany, P.; Alvarez, S. *Inorg. Chem.* **2013**, *52*, 6510.

- (40) Maleckis, A.; Sanford, M. S. *Organometallics* **2011**, *30*, 6617; Canty, A. J.; Minchin, N. J.; Skelton, B. W.; White, A. H. *J. Chem. Soc., Dalton Trans.* **1986**, 2205; Tsuji, S.; Swenson, D. C.; Jordan, R. F. *Organometallics* **1999**, *18*, 4758; Guzei, I. A.; Li, K.; Bikzhanova, G. A.; Darkwa, J.; Mapolie, S. F. *Dalton Trans.* **2003**, 715; Yamashita, M.; Takamiya, I.; Jin, K.; Nozaki, K. *J. Organomet. Chem.* **2006**, *691*, 3189; Anezaki, S.; Yamaguchi, Y.; Asami, M. *J. Organomet. Chem.* **2011**, *696*, 2399; Togni, A.; Burckhardt, U.; Gramlich, V.; Pregosin, P. S.; Salzmann, R. *J. Am. Chem. Soc.* **1996**, *118*, 1031.
- (41) Tan, R.; Jia, P.; Rao, Y.; Jia, W.; Hadzovic, A.; Yu, Q.; Li, X.; Song, D. *Organometallics* **2008**, *27*, 6614; Tan, R.; Song, D. *Dalton Trans.* **2009**, 9892.
- (42) Cano, J.; Royo, P.; Lanfranchi, M.; Pellinghelli, M. A.; Tiripicchio, A. *Angew. Chem. Int. Ed.* **2001**, *40*, 2495.
- (43) Borodkin, G. I.; Nagi, S. M.; Bagryanskaya, I. Y.; Gatilov, Y. V. *Russ. J. Struct. Chem.* **1984**, *25*, 114; Davlieva, M. G.; Lindeman, S. V.; Neretin, I. S.; Kochi, J. K. *J. Org. Chem.* **2005**, *70*, 4013; Baezinger, N. C.; Nelson, A. D. *J. Am. Chem. Soc.* **1968**, *90*, 6602; Hubig, S. M.; Lindeman, S. V.; Kochi, J. K. *Coord. Chem. Rev.* **2000**, *200*, 831; Borodkin, G. I.; Nagi, S. M.; Gatilov, Y. V.; Shakirov, M. M.; Rybalova, T. V.; Shubin, V. G. *Russ. J. Org. Chem.* **1992**, *28*, 1806; Musso, F.; Solari, E.; Floriani, C.; Schenk, K. *Organometallics* **1997**, *16*, 4889; Kraft, A.; Beck, J.; Steinfeld, G.; Scherer, H.; Himmel, D.; Krossing, I. *Organometallics* **2012**, *31*, 7485; Zaworotko, M. J.; Cameron, T. S.; Linden, A.; Sturge, K. C. *Acta Cryst., Sect. C: Cryst. Struct. Commun.* **1989**, *45*, 996; Borodkin, G. I.; Gatilov, Y. V.; Nagi, S. M.; Shubin, V. G. *Russ. J. Struct. Chem.* **1996**, *37*, 234; Reed, C. A.; Kim, K.-C.; Stoyanov, E. S.; Stasko, D.; Tham, F. S.; Mueller, L. J.; Boyd, P. D. W. *J. Am. Chem. Soc.* **2003**, *125*, 1796; Schafer, A.; Reissmann, M.; Schafer, A.; Saak, W.; Haase, D.; Muller, T. *Angew. Chem. Int. Ed.* **2011**, *50*, 12636.
- (44) Alvarez, M. A.; García, M. E.; García-Vivo, D.; Menéndez, S.; Ruiz, M. A. *Organometallics* **2013**, *32*, 218; Bambirra, S.; Meetsma, A.; Hessen, B. *Organometallics* **2006**, *25*, 3454.
- (45) *Gaussian09* (B.1), Frisch, M. J. et al., Gaussian, Inc., Wallingford, CT, 2010.
- (46) Dimitrios, A. D.; Chem, X.-Y.; Landis, C. R.; Neese, F. *J. Chem. Theory Comput.* **2008**, *4*, 908.
- (47) Keith, T.A. AIMAll (Version 10.12.08), TK Gristmill Software, Overland Park KS, USA, **2010** (aim.tkgristmill.com).